ELECTRON BEAM TEMPERATURE MEASUREMENTS AT THE FERMILAB MEDIUM ENERGY ELECTRON COOLER*

A. Warner#, K. Carlson, L. Prost, M. Sutherland FNAL, Batavia, IL 60510, U.S.A.
G. Kazakevich, BINP, 630090 Novosibirsk, Russia

Abstract

The Fermilab Recycler ring employs an electron cooler to store and cool 8.9-GeV anti-protons. The cooler is based on an electrostatic accelerator (Pelletron) working in an energy-recovery regime [1]. Several techniques for determining the characteristics of the beam dynamics have been investigated. Beam temperature measurements using optical transition radiation (OTR) [2],[3], in conjunction with a Pepper-pot have been made at several settings of the upstream optics of the machine. Without temperature the pepper-pot hole images would have sharp boundaries. A finite temperature makes these boundaries broader. Thus, comparison of the ratios of the hole image boundaries and intensities is a measure of the beam temperature. In this paper we report the results so far obtained using this technique.

INTRODUCTION

Electron cooling of the anti-protons in the Recycler requires that a monochromatic (cold) electron beam be transported to a common 20 meter long cooling section to interact with the stored anti-protons. The cooling efficiency strongly depends on the effective angle between these electrons and the anti-protons. Hence, to have optimal cooling, the electron rms angle should be as small as possible. Several sources including the source temperature contribute to the total rms angle. As a result, optimization of the cooling process places an upper limit on the contribution to the total angle due to beam temperature. A significant effort was made to determine this contribution by analyzing images of the electron beam taken with optical transition radiation monitors in conjunction with a pepper-pot scraper. The main parameters of the cooler are summarized in table 1.

Table 1: Electron Cooler Main Parameters

Parameter	Symbol	Value	Unit
Electron kinetic energy	E_b	4.34	MeV
Beam current	I_b	0.1-0.5	A
High voltage ripple, rms	δU	250	V
CS length	L	20	m
Solenoid field in CS	B_{cs}	105	G
Beam radius in CS	R_b	3-4.5	mm

EXPERIMENTAL SET-UP

The Recycler Electron cooler is equipped with a so-called pepper-pot (PP), installed downstream of the acceleration tube right above the first bending magnet as shown in Figure 1. The PP is a copper plate with 475 equally spaced (0.81 mm center-to center), 0.27 mm-diameter round holes which have been designed to form a square grid pattern. The density of holes is sufficient to cover the smallest beam diameter of ~ 5 mm at the PP location by 5 holes. When inserted and used with a 2-μs pulsed electron beam the PP blocks the beam allowing only beamlets (small beams) to pass through the holes. These beamlets can vary in number from a few to several dozen depending on the focusing and the beam current. The beamlets that pass through are observed on a down stream OTR monitor and CCD camera system.

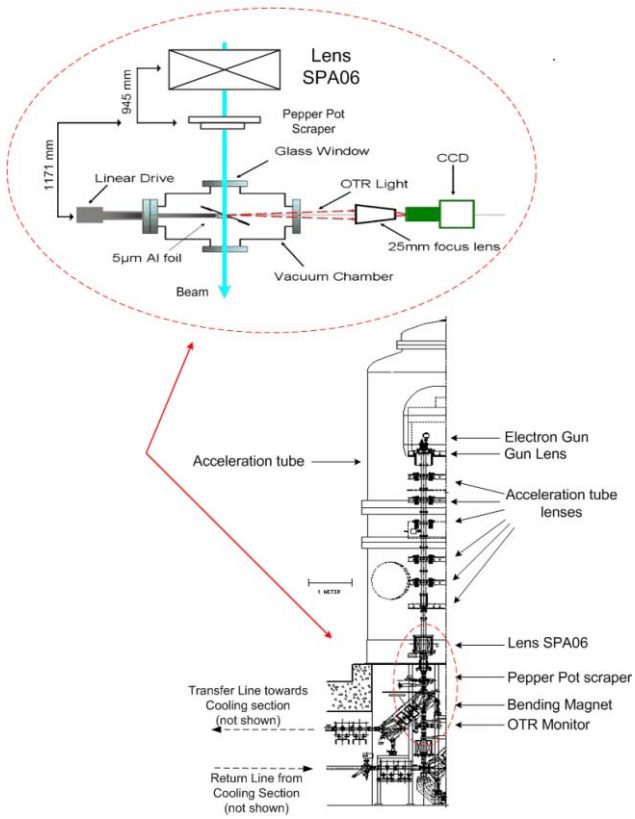

Figure 1: Layout of experimental set-up.

The transition radiation screen is a 5μm, 2-inch diameter aluminum foil tensioned onto a ring frame. Such thin foils were used to reduce the background signal due to beam scattering and bremsstrahlung radiation. The response of the monitors as a function of the beam current shows good linearity over the practical range of the cooler (Figure 2) and the light output is very uniform over the surface of the monitor. A linear motor drive inserts the OTR screen in the beam path with an accuracy of 0.1 mm and the screen is at an angle of 38.9 degrees with respect

*Operated by Fermi Research Alliance, LLC under Contract No. DE-AC02-07CH11359 with the United States Department of Energy.
#warner@fnal.gov

to the beam direction. This corresponds to the angle $\theta \approx 1/\beta\gamma$ [4], where the intensity of the light is at a maximum.

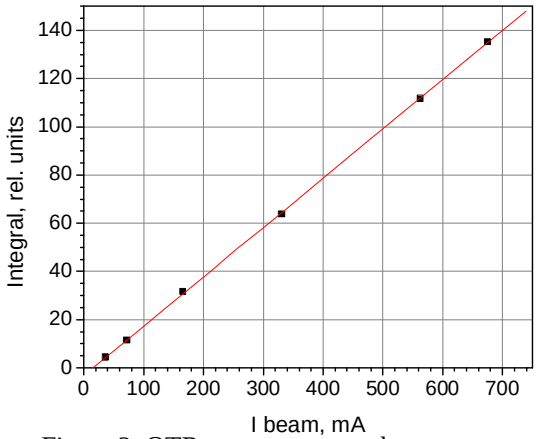

Figure 2: OTR response versus beam current.

Principle of Measurement

In the ideal case of a linear axially symmetric distribution of the electron angles, the hole pattern produced by the beamlets at the OTR should be undistorted and therefore image analysis would allow one to measure both quadrupole and non-linear aberrations in the beam angles. In other words a beam without temperature would have sharp boundaries; however, due to finite temperature these boundaries are broadened. Thus comparison of the widths of the hole images with that of the scraper is a measure of the beam temperature. Likewise comparison of the imaged intensity from the PP is also a measure of the temperature. Due to temperature, the image intensity of a beamlet on the OTR screen can be represented as $\propto \exp(-r^2/(2\sigma^2))$, where r is the distance from the image center, and the width σ depends on the thermal emittance and optical functions [5]. If the beam is round at the scraper and there are no optical elements between the scraper and the OTR detector, the width of the point image is given by:

$$\sigma = \frac{p_T a_g}{p a_o} l \qquad (1)$$

Where p is the total momentum, $p_T = \sqrt{m_e T}$ is the transverse momentum due to thermal motion, a_g is the cathode radius, a_0 is the beam radius at the scraper and l is the distance between the scraper and the OTR detector. Equation (1) can be rewritten in term of the ratio of the intensities [5] as:

$$\frac{I_i}{I_0} = \frac{\rho^2}{\sigma^2} = \frac{\rho^2}{2\theta_T^2 l^2} \qquad (2)$$

Where I_i is the intensity of a beamlet at position (x_i, y_i), I_0 is the intensity of the full beam, θ_T is the transverse momentum due to thermal motion and ρ is the PP hole radius. To prevent loss of image brightness the PP holes has to be wide enough, such that the radius of the hole be much larger than the hole depth.

Data Acquisition

The optical monitor system uses digital CCD cameras connected via IEEE 1394 (fire-wire) standards to computers; the images are first converted to optical signals in order to transport the data over longer distances. At the interface to the computer the signal is converted back to 1394 standard input. A LabView™ based application program that was designed using commercially developed image analysis tools is used to process the data. The system incorporates image digitization, image display, as well as image analysis and system calibration in a real-time module. The gain and other attributes of the camera are controlled via this interface as well.

Data Analysis

First, linear (convolution) filters are applied to the images in order to remove unwanted background due to x-rays. Then, the images are scaled to reflect real world coordinates and corrected for angular errors and aberrations due to tilts or camera misalignment. The correction to the beam image shape due to the angle of the OTR foil (38.9°) is ~ 20 pixels/mm horizontally and ~ 16 pixels/mm vertically. The CCDs chosen are square pixel CCDs so that there is no need to convert the aspect ratio during the processing. Measurements of the beam centers, the rms beam size and the ratio of the intensity of the images are determined using the image analysis tools.

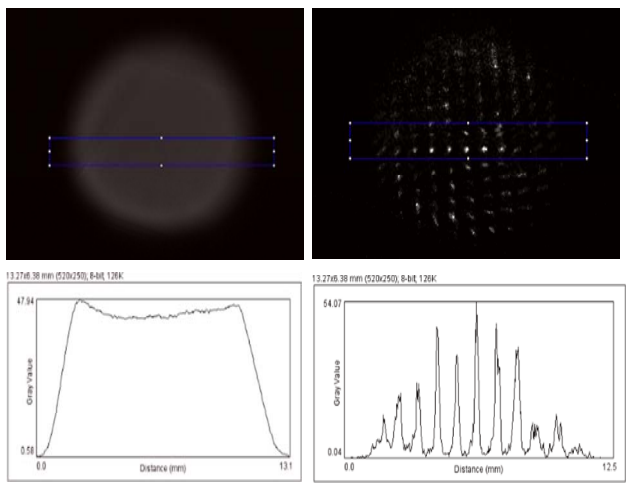

Figure 3: Top left: OTR image, Top right: PP image Bottom left: ROI integral, Bottom right: ROI PP image.

Figure 3 shows a processed data set where the beam (top left) and the corresponding PP image (top right) are measured and the relative grey scale intensities are used to determine θ_T from equation (2). The data shown was taken

for fixed optics upstream of the OTR monitor and for a pulsed beam current of ~ 900 mA. The integral over a specified region of interest (ROI) is also shown in Figure 3 (bottom left and bottom right) for the beam and its PP image. The current emitted during a pulse is controlled by varying the pulse voltage of the gun control electrode; to compensate for pulser and optics variations during the rise of the pulse, data from 1μs beam pulses are subtracted from 2 μs beam pulses, such that only the flat-top-equivalent image remains. The shape of the pulse-signal is shown in Figure 4. The PP data shown was scaled by a multiplicative factor to enhance the image of the beamlets for data processing. The scaling factors were taken care of when the ratios of the image intensities were determined.

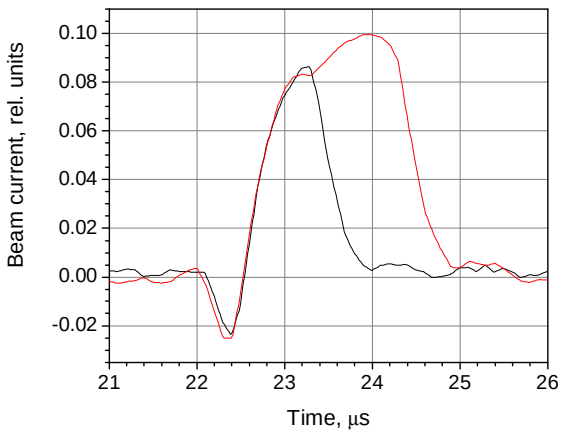

Figure 4: Pulse signal shape at 1 μs and 2 μs.

RESULTS

The results of the measurements are summarized in Table 2. Using Eq. (1) and (2), we find that thermal angles are ~71 μrad ≈ ≃ 0.45 eV. As mentioned previously several sources contribute independently to the total rms angle, including imperfections of the magnetic field (< 100 μrad), perturbations from external fields (~ 40 μrad), and envelope oscillations (estimated at ~ 120 μrad) [6]. These angles are added in quadrature.

Table2: Measurement Results

Parameter	Symbol	Value	Unit
PP to OTR distance	l	1171	mm
Cathode radius	a_g	3.8	mm
Beam radius	a_o	5.7	mm
Total momentum	p	4.8	MeV/c
Thermal angle	θ_T	71	μrad
Thermal momentum	P_T	504	eV
Beam Temperature	T	0.45	eV

ACKNOWLEDGEMENTS

The authors are thankful to A. Burov and A. Shemyakin for their useful discussions and for the analytical work that was done in the design of the pepper-pot scraper. We also wish to acknowledge Charles Schmidt for his participation in the data collection and R. Kellett for his technical assistance during the hardware installation.

SUMMARY

The measured thermal angle is within the tolerance of the design goal and the total rms angle meets the goal of < 0.2 mrad. The resultant electron beam quality achieved lead to successful cooling up to 400 × 10^{10} antiprotons.

Table 2: Summary of electron angles in the cooling section

Component	Design μrad	Present estimation μrad	Diagnostics
Temperature	90	70	OTR + PP
Aberrations	90	50 ≤30 (@ 1 mm)	Simulated BPMs
Envelope scalloping	100	120	Movable orifices
Dipole motion caused by magnetic field imperfections	100	40	Magnetic measurements + BPMs
Beam motion	50	40	BPMs
Drift velocity	20	20	Calculated
Total	**200**	**160**	

REFERENCES

[1] S. Nagaitsev et al, Phys. Rev. Lett. 96, 044801 (2006).

[2] L. Wartski et al, "Interference phenomenon in optical transition radiation and its application to particle beam diagnostics and multiple-scattering measurements," J. Appl. Phys., vol. 46, no. 8, pp. 3644-3653, 1975.

[3] V. L. Ginzburg and I. M. Frank, "Radiation from a uniformly moving electron passing from one medium to another,." J. Exp. Theoret. Phys., Vol. 16, no. 15, pp. 15-26, 1946.

[4] A. Warner et al, "Beam profile diagnostics for the Fermilab Medium Energy Electron Cooler. " IEEE Trans. Nucl. Sci,V. 52, no. 5, 2005.

[5] A. Burov and A. Shemyakin, "Pepper-pot Scraper Parameters and Data Processing ," Fermilab-TM-2258, July 2004.

[6] A. Burov *et al.*, AIP Conf. Proc. Vol. 821 (2006) 139.